Comparison of density functionals for energy and structural differences between the high- $[^5T_{2g}:(t_{2g})^4(e_g)^2]$ and low- $[^1A_{1g}:(t_{2g})^6(e_g)^0]$ spin states of the hexaquoferrous cation $[Fe(H_2O)_6]^{2+}$

Antony Fouqueau, Sébastien Mer, and Mark E. Casida[a)]
Institut de Chimie Moleculaire de Grenoble (ICMG, FR-2607), Laboratoire d'Études Dynamiques et Structurales de la Sélectivité (LÉDSS, UMR 5616), Équipe de Chimie Théorique (LÉDSS-ÉCT), Université Joseph Fourier (Grenoble I), F38041 Grenoble, France

Latevi Max Lawson Daku and Andreas Hauser
Département de Chimie Physique, Laboratoire de Photophysique et Photochimie des Composés de Métaux de Transition, Université de Genève, 30 quai Ernest-Ansermet, CH-1211 Genève 4, Switzerland

Tsonka Mineva
Institute of Catalysis, Bulgarian Academy of Sciences, 1113 Sofia, Bulgaria

Frank Neese
Max Planck Institut für Bioanorganische Chemie, Stiftstrasse 34-36, Mülheim an der Ruhr 45470, Germany

(Received 24 April 2003; accepted 27 February 2004)

A comparison of density functionals is made for the calculation of energy and geometry differences for the high- $[^5T_{2g}:(t_{2g})^4(e_g)^2]$ and low- $[^1A_{1g}:(t_{2g})^6(e_g)^0]$ spin states of the hexaquoferrous cation $[Fe(H_2O)_6]^{2+}$. Since very little experimental results are available (except for crystal structures involving the cation in its high-spin state), the primary comparison is with our own complete active-space self-consistent field (CASSCF), second-order perturbation theory-corrected complete active-space self-consistent field (CASPT2), and spectroscopy-oriented configuration interaction (SORCI) calculations. We find that generalized gradient approximations (GGAs) and the B3LYP hybrid functional provide geometries in good agreement with experiment and with our CASSCF calculations provided sufficiently extended basis sets are used (i.e., polarization functions on the iron and polarization and diffuse functions on the water molecules). In contrast, CASPT2 calculations of the low-spin–high-spin energy difference $\Delta E_{LH}=E_{LS}-E_{HS}$ appear to be significantly overestimated due to basis set limitations in the sense that the energy difference of the atomic asymptotes ($^5D\rightarrow{}^1I$ excitation of Fe^{2+}) are overestimated by about 3000 cm^{-1}. An empirical shift of the molecular ΔE_{LH} based upon atomic calculations provides a best estimate of 12 000–13 000 cm^{-1}. Our unshifted SORCI result is 13 300 cm^{-1}, consistent with previous comparisons between SORCI and experimental excitation energies which suggest that no such empirical shift is needed in conjunction with this method. In contrast, after estimation of incomplete basis set effects, GGAs with one exception underestimate this value by 3000–4000 cm^{-1} while the B3LYP functional underestimates it by only about 1000 cm^{-1}. The exception is the GGA functional RPBE which appears to perform as well as or better than the B3LYP functional for the properties studied here. In order to obtain a best estimate of the molecular ΔE_{LH} within the context of density functional theory (DFT) calculations we have also performed atomic excitation energy calculations using the multiplet sum method. These atomic DFT calculations suggest that no empirical correction is needed for the DFT calculations. © *2004 American Institute of Physics.*
[DOI: 10.1063/1.1710046]

I. INTRODUCTION

A well-known feature of d^6 Tanabe–Sugano ligand field theory (LFT) diagrams for octahedral complexes is the reversal of the ordering of the low-spin ^1A and high-spin ^5T in the spin-crossover region of ligand field strength.[1] For compounds in this region, spin crossover may be either thermally or optically induced,[2] leading to possible applications in storage and display devices.[3–5] We are particularly interested in the phenomenon of light-induced excited spin-state trapping (LIESST) in octahedral iron II compounds, which involves the optical interconversion of the high-spin (HS) $^5T_{2g}$ and low-spin (LS) ^1A_g electronic states. While this can be understood at a qualitative level using LFT,[1,2] it is also known that the e_g orbitals, populated in going from the LS to the HS state, are antibonding, so that bonds are longer in the HS than in the LS state. This change in geometry results in a change of ligand field which is difficult to take into account quantitatively in simple LFT. Hence theoretical treatments which go beyond LFT are needed for a detailed treatment of spin crossover and LIESST in particular. In this article we examine the performance of various density functionals for

a)Electronic mail: Mark.Casida@ujf-grenoble.fr

describing the HS and LS geometries and energetics of the hexaquoferrous cation $[Fe(H_2O)_6]^{2+}$. Since water is a weak-field ligand, hexaquoferrous cation is quite far from the interesting spin-crossover region. However, it is interesting as a "textbook example" of an octahedral ferrous compound and provides a useful preliminary for future studies of octahedral ferrous compounds which do exhibit LIESST.

To our knowledge, there has been only a few previous applications of density-functional theory (DFT) to spin crossover in octahedral ferrous compounds.[6–11] Those aspects of these studies which are pertinant to an investigation of functionals will be reviewed in the next section. Suffice it to say that they all involve calculations on molecules which are too large to allow comparison against detailed *ab initio* calculations. As such, we do not yet have a general calibration on a variety of simple octahedral ferrous compounds on which to draw firm conclusions as to what quality of HS and LS geometries and energies should be expected in general from a given level of density-functional approximation. By examining a far simpler compound—namely, $[Fe(H_2O)_6]^{2+}$—where detailed *ab initio* calculations can be performed, we hope to be able to begin to provide the necessary background data for a general assessment of functionals.

It should probably be pointed out that the issue of whether density functionals should be assessed by comparison against experimental data or against the results of *ab initio* calculations is not entirely clear. Although it might seem that the most direct comparison of results from gas-phase zero-temperature DFT calculations should be with the results of gas-phase zero-temperature *ab initio* calculations, rather than with the condensed-phase finite-temperature experimental data which are typically available for the compounds of interest here, calculations of $3d$ transition-metal complexes are far from trivial, primarily because of the large amount of electron correlation created by the pseudodegeneracy of the $4s$ and $3d$ orbitals. Often the best *ab initio* treatments seem to require empirical corrections to give "best estimates" in order to approach an accuracy better than 5 kcal/mol (1750 cm^{-1}).[12,13] This is an immense error when compared with the HS–LS energy difference of 100 cm^{-1} typical in compounds exhibiting the LIESST phenomenon and places a distinct limitation on how well we can expect to be able to assess density functionals for describing this phenomenon. Nevertheless, *ab initio* and DFT calculations remain our most reliable theoretical models for the overall behavior of these compounds and, when used with suitable care and consciousness of the limitations inherent in these models, should provide an important complement to LFT. It is our objective to establish just what type of care is needed and where lie the numerical limitations of the theory. The *ab initio* methods used here are well established and can now be said to be fairly well understood. We find that the principal limitation of *ab initio* methods is to underestimate dynamic correlation, leading to an overestimate of the differences between the LS and HS states, leading to similar results from the different *ab initio* methods we have considered. Note, however, that the difference-dedicated configuration interaction method is an exception to this rule since it is deliberately designed to give a balanced cancellation of errors between the ground and excited states.[14,15] The difference dedicated configuration interaction philosophy was also used in the design of the recently developed spectroscopy-oriented configuration interaction (SORCI) procedure.[16] This method is an efficient multireference-variation–perturbation approach which focuses on the calculation of energy differences between several states of possibly different multiplicity within an individually selecting configuration interaction strategy. As far as DFT is concerned, it seems fair to say that the behavior of different density functionals seems to be less well understood, particularly when it comes to specific types of applications such as the spin transitions which interest us. For this reason and because most LIESST compounds are simply too large to treat adequately with traditional *ab initio* methods, our emphasis will be on determining the limitations of present-day density functionals. In this way, we hope to foresee and avoid carrying out expensive calculations whose "theoretical error bars" are too big to address the questions being asked.

In this context, we also note a study somewhat similar to our own but for $[Fe(H_2O)_6]^{3+}$ (Ref. 17). Harris, Loew, and Kormornicki found that DFT, with a suitably chosen functional, could compete with *ab initio* theory and that semiempirical ZINDO excitation energies *obtained at DFT optimized geometries* were in excellent agreement with experiment.

Our paper is divided into the following sections: Some of the issues which distinguish different functionals of interest for applications to spin-crossover ferrous compounds are reviewed in the next section. The technical details of our calculations are given in Sec. III. In Sec. IV, we give our results. We consider first optimized geometries, followed by a comparison of HS and LS complex energies. This comparison of energies also involves the atomic limit—i.e., at the Fe^{2+}-atom ^5D ground and ^1I excited states, not only because of the spectroscopic importance of knowing the separated complex limit of our potential energy surfaces, but also because very detailed experimental data are available for the atom which might be used as an additional criterium for assessing density functionals. The multiplet sum method used to estimate DFT excitation energies is briefly discussed in the Appendix. Section V summarizes.

II. DENSITY FUNCTIONALS

Since our objective is the evaluation of density functionals for spin-crossover compounds, it is necessary to say a few words about the functionals which were considered in this paper. More general background information about DFT may be found in Refs. 18–20.

Most modern DFT calculations are carried out in a modified Kohn–Sham formalism[21] where the total electronic energy is written (in hartree atomic units) as

$$E=\sum_{i\sigma} n_{i\sigma}\langle\psi_{i\sigma}|\hat{h}_{\mathrm{core}}|\psi_{i\sigma}\rangle + \frac{1}{2}\int\int\frac{\rho(\mathbf{r})\rho(\mathbf{r}')}{|\mathbf{r}-\mathbf{r}'|}d\mathbf{r}'+E_{\mathrm{xc}}[\rho_\uparrow,\rho_\downarrow], \tag{2.1}$$

where $n_{i\sigma}$ is the occupation number of the Kohn–Sham orbital $\psi_{i\sigma}$, $\hat{h}_{\text{core}}$ is the usual core Hamiltonian, and the spin-up, spin-down, and total charge densities are given by

$$\rho_\sigma(\mathbf{r}) = \sum_i n_{i\sigma} |\psi_{i\sigma}(\mathbf{r})|^2,$$
$$\rho(\mathbf{r}) = \rho_\uparrow(\mathbf{r}) + \rho_\downarrow(\mathbf{r}). \tag{2.2}$$

The exchange-correlation energy is often written in terms of the exchange-correlation energy density per particle:

$$E_{\text{xc}}[\rho_\uparrow, \rho_\downarrow] = \int \rho(\mathbf{r}) \epsilon_{\text{xc}}[\rho_\uparrow, \rho_\downarrow](\mathbf{r}) d\mathbf{r}. \tag{2.3}$$

The local density approximation[21] (LDA) consists of the assumption that

$$\epsilon_{\text{xc}}^{\text{LDA}}[\rho_\uparrow, \rho_\downarrow](\mathbf{r}) = \epsilon_{\text{xc}}^{\text{HEG}}(\rho_\uparrow(\mathbf{r}), \rho_\downarrow(\mathbf{r})), \tag{2.4}$$

where the universality of the exchange-correlation functional is used to justify the use of ϵ_{xc} for the homogeneous electron gas (HEG). Calculations reported in this paper use the Vosko–Wilk–Nusair parametrization for the LDA correlation energy[22] (the VWN5, *not* the VWN, option in GAUSSIAN), except where we have used the exchange-only variant of the LDA known as $X\alpha$. The full (exchange +correlation) LDA works remarkably well for the calculation of molecular ionization potentials, equilibrium geometries, and vibrational frequencies. It does this by underestimating exchange by about 14% and overestimating correlation by a factor of about 2.5 in such a way that the two errors tend to cancel (Ref. 19, p. 231). One might think that an approximation which underestimates exchange by more than 10% would lead to serious errors in describing the parallel spin (i.e., Fermi) correlation. In particular, it is often reasoned that the lower-energy state of two states differing only in their number of unpaired electrons is always that with more parallel-spin electrons since Fermi correlation keeps the parallel-spin electron pairs spatially separated, thereby reducing the electron repulsion energy. Thus an error in the DFT description of exchange may be expected to lead to an underestimation of the splitting between these states of different spin multiplicity (in cases where the HS state is lower in energy than the LS state).

An important drawback of the LDA is that it tends to overbind molecules. This drawback was corrected by the discovery of generalized gradient approximations (GGAs), which incorporate the gradient of the charge density in order to improve the description of the exchange-correlation energy in the ''boundary region'' at the outer edges of atoms and where molecular binding occurs.[23] The general formula is particularly simple for the exchange part,

$$\epsilon_x^{\text{GGA}}[\rho_\uparrow, \rho_\downarrow](\mathbf{r}) = \sum_\sigma \epsilon_x^{\text{HEG}}(\rho_\sigma(\mathbf{r}))[1 + F(\rho_\sigma(\mathbf{r}), x_\sigma(\mathbf{r}))], \tag{2.5}$$

where the enhancement factor F depends upon the reduced gradient:

$$x_\sigma(\mathbf{r}) = \frac{|\vec{\nabla}\rho_\sigma(\mathbf{r})|}{\rho^{4/3}(\mathbf{r})}. \tag{2.6}$$

An example in the present work is Becke's 1988 exchange-only GGA (B) (Ref. 24). Expressions for correlation GGAs are complicated, among other things, by a different spin dependence. We have used both Perdew's 1986 correlation GGA (P86) (Ref. 25) and the GGA correlation functional of Lee, Yang, and Parr (LYP) (Ref. 26). The combination B+P86 is referred to as BP86 while the combination B+LYP is referred to as BLYP. More modern GGAs have been developed without separating exchange and correlation. We have used the 1991 exchange-correlation GGA of Perdew and Wang (PW91) (Ref. 27), the 1997 exchange-correlation GGA of Perdew, Burke, and Ernzerhof (PBE) (Ref. 28), as well as the revised PBE (RPBE) of Hammer, Hansen, and Nørskov (Ref. 29). These latter GGAs have been carefully designed to satisfy as many as possible of the known conditions which should be satisfied by the exact exchange-correlation functional. It is natural to expect that GGA exchange is also underestimated with respect to the true exchange since GGA exchange is dominated by its LDA component. Thus GGAs might also be expected to give artificially small splitting energies between states of different spin multiplicities.

By 1993, GGAs seemed to have reached the limit of what they could do for thermochemistry. In order to go beyond this limit, Becke[30] introduced the idea of a hybrid functional by using the adiabatic connection formalism of Harris and Jones[31] in which the electron repulsion $\lambda \hat{v}_{ee}$ for $\lambda = 1$ is gradually turned on in the presence of a compensating potential $\hat{w}_\lambda[\rho_\uparrow, \rho_\downarrow]$, which keeps the density fixed. For any given value of λ,

$$(\hat{h}_{KS} + \lambda \hat{v}_{ee} + \hat{w}_\lambda[\rho_\uparrow, \rho_\downarrow])\Psi_\lambda = E_\lambda \Psi_\lambda. \tag{2.7}$$

At $\lambda = 0$, there is no electron repulsion, so we have the Kohn–Sham fictitious system of noninteracting electrons whose wave function $\Psi_{\lambda=0}$ is a single determinant. At $\lambda = 1$, we have the fully interacting real system. This way of adiabatically connecting the Kohn–Sham and real systems allows us to write that

$$E_{\text{xc}} = \int_0^1 E_{\text{xc}}^\lambda d\lambda. \tag{2.8}$$

The single-determinant nature of $\Psi_{\lambda=0}$ tells us that

$$E_{\text{xc}}^{\lambda=0} = E_x. \tag{2.9}$$

Perdew, Ernzerhof, and Burke[32] have suggested the ansatz that

$$E_{\text{xc}}^\lambda = E_{\text{xc}}^{\lambda=1} + (1-\lambda)^{n-1}(E_x^{\lambda=0} - E_x^{\lambda=1}), \tag{2.10}$$

where $n = 4$ is chosen on the basis of fourth-order Møller–Plesset perturbation theory. This then leads to

$$E_{\text{xc}} = E_{\text{xc}}^{\lambda=1} + \frac{1}{4}(E_x^{\lambda=0} - E_x^{\lambda=1}). \tag{2.11}$$

If we then reason (as did Becke[30]) that $E_x^{\lambda=0}$ should be well approximated by Hartree–Fock exchange E_x^{HF}, while GGAs should best describe $E_x^{\lambda=1}$ and $E_{\mathrm{xc}}^{\lambda=1}$, we arrive at hybrid functionals with the formula

$$E_{\mathrm{xc}}^{\mathrm{hybrid}}=E_{\mathrm{xc}}^{\mathrm{GGA}}+\frac{1}{4}(E_x^{\mathrm{HF}}-E_x^{\mathrm{GGA}}). \tag{2.12}$$

In practice, the best known hybrid functional and the one we use here is the B3LYP functional[33] defined by

$$E_{\mathrm{xc}}=(1-a_0)E_x^{X\alpha}+a_0E_x^{\mathrm{HF}}+a_xE_x^{\mathrm{B}}+a_cE_c^{\mathrm{LYP}} +(1-a_c)E_c^{\mathrm{VWN}}, \tag{2.13}$$

where $a_0=0.20$, $a_x=0.72$, and $a_c=0.81$. In agreement with the ideas of Perdew, Ernzerhof, and Burke,[32] $a_0\approx 1/4$ and $a_x\approx 3/4$.

One might expect the estimate of Fermi correlation to be improved in going from GGAs to hybrid functionals because of the inclusion of some Hartree–Fock (HF) exchange, thus increasing and so improving the splitting between states of different spin multiplicities. In fact, Paulsen *et al.*[6] have examined the ability of the BLYP and PW91 generalized gradient functionals and the B3LYP hybrid functional to predict the spin-crossover transition temperature of substituted and unsubstituted di[*tris*-(1-pyrazolyl)methane] ferrous cation $[\mathrm{Fe(tpm)_2}]^{2+}$. They noticed that the B3LYP significantly stabilized the HS state, making it lower in energy than the LS state, contrary to what is observed experimentally. Interestingly the same preference for a low-multiplicity ground state seen in nature for this compound was also found with the GGAs. At about the same time Reiher, Salomon, and Hess[7] confirmed that the B3LYP functional stabilizes the HS state with respect to the LS state more than do GGA functionals in an examination of the ability of various density functionals to predict the experimentally observed HS–LS splitting in the Fe(II) spin-crossover complexes with sulfur-containing ligands of around 30 atoms. They found that the GGA BP86 (but also the GGA PBE and the hybrid PBE0) very much underestimated the HS–LS energy difference, but that the hybrid functional B3LYP gave much more reasonable values. This then led them to propose[7,9,10] the B3LYP* functional, which differs from the B3LYP functional only in that the amount of HF exchange is reduced ($a_0=0.15$) to give a better fit of calculated and experimental HS–LS energy differences. The B3LYP* functional was further tested in Ref. 9, in particular for the HS–LS splittings in metallocenes and in bis(benzene) metal complexes of the first transition-metal period, and found to be a dramatic improvement over the B3LYP functional alone for the calculation of HS–LS energy differences, without important changes in the prediction of other proper properties. This behavior has been further confirmed by Reiher in a study of the spin-crossover compound $\mathrm{Fe(phen)_2(NCS)_2}$ using the GGAs BP86 and BLYP and the hybrid functionals B3LYP and B3LYP* (Ref. 10).

While reparametrizing the B3LYP functional is certainly an appealing simple approach to the problem, it does have a few drawbacks. First of all, it would be nice to have a universal functional good for all properties. It is much easier to reparametrize a functional for one property and a limited class of compounds than to obtain a functional which will work for all properties and all compounds. Reiher[10] points out that the B3LYP* functional is not necessarily optimal for the calculation of properties other than the HS–LS energy difference and in particular is not recommended for the calculation of vibrational energies. Furthermore, he recommends the BP86 functional for the calculation of the transition temperature in spin-crossover complexes because of a subtle cancellation of errors between the vibrational and electronic contributions to the overall energy difference. (In particular, BP86 *harmonic* frequencies agree better with experimental frequencies *which include anharmonic effects* than do B3LYP *harmonic* frequencies.[34] Thus there is a useful error in the BP86 frequencies which does not seem to be shared with those generated with the B3LYP functional.) This preference for a GGA over a hybrid functional for the calculation of HS–LS energy differences *which include vibrational effects* is also seen in the work of Paulsen *et al.*[6] who obtained best agreement with experiment by using the PW91 functional. Most recently Baranović[11] has examined the theoretical prediction of the equilibria of the HS and LS Fe(II) spin-crossover complexes $\mathrm{Fe(1,10\text{-}phenanthroline)_2(NCS)_2}$, $[\mathrm{Fe(2\text{-}picolylamine)_3}]^{2+}$, and $[\mathrm{Fe(bis(1,4,7\text{-}triazacyclononane))_2}]^{2+}$ with the BP86 functional and has found excellent agreement with experiment after the introduction of appropriate scaling parameters.

In fact, even the very arguments upon which is based the B3LYP* functional could be called into question. For example, Levine in his popular textbook points out that the traditional explanation of Hund's rule (given above) turns out to be wrong in most cases (though the conclusion is correct) and that the actual reason has more to do with the indirect reduction of electron–nucleus screening by Pauli repulsion (Ref. 35, pp. 328–329). Furthermore, the quality of DFT calculations of $i\rightarrow a$ singlet $(i\uparrow i\downarrow)$–triplet $(i\uparrow a\uparrow)$ excitation energies for organic molecules is well established and GGAs give quite reasonable values. Could the situation actually be more complicated than it first appears? Koch and Holthausen (Ref. 20, pp. 173–176) have reviewed different functionals for the calculation of the energy difference between the lowest-lying singlet and triplet states of carbenes and related species. This is a case where HF calculations fail rather badly because the singlet state is strongly dominated by two nearly degenerate determinants. Hybrid functionals (B3LYP, B3P86, and B3PW91 in the particular case of methylene) do better, but are still rather far from experiment as are some GGAs (BP86 and BPW91 for methylene). On the other hand, it is only the GGA functionals BVWN and BLYP which come within 1 kcal/mol of the experimental value of the $^1A_1$–$^3B_1$ energy gap in methylene. The authors' conclusion is that in this case, "pure density functionals are usually to be preferred over hybrid ones." Of course, this is a case where it could be argued that the BVWN and BLYP functionals give too high an energy for the singlet state because they do not take static correlation properly into account and give too high an energy for the triplet state for the reasons already mentioned. Thus the errors compensate. Nevertheless, it may be taken as a warning that the arguments in favor

of hybrid functionals over GGAs for calculating the relative energies of different spin states, while compelling from a heuristic point of view, are certainly not always easy to generalize. In fact, it has not yet been estabished that a GGA will never do as well as a hybrid functional for this property. In the remainder of this paper we compare the BP86, PW91, PBE, RPBE, BLYP, and B3LYP functionals against high-quality *ab initio* calculations and experiment for the characterization of the LS and HS states of the hexaquo ferrous cation.

III. COMPUTATIONAL DETAILS

A. *Ab Initio* calculations

Our choice of *ab initio* methods has been at least partially the result of attempting to seek the best compromise been the competing needs to use extensive basis sets and to include an accurate description of electron correlation. After some experimentation, we chose to focus on carrying out the best possible complete active space self-consistant field (CASSCF) with second-order perturbative correction (CASPT2) within the means at our disposal. The CASPT2 method has been compared with time-dependent density-functional theory and other *ab initio* methods by Daniel in a recent review[36] concerning what type of accuracy is now achievable for excitations in transition-metal coordination compounds. The CASPT2 method is certainly one of the methods of choice. Estimates of its accuracy vary, but typical errors are on the order of a few tenths of an eV (i.e., a few thousand cm^{-1}).[37] This is also typical of what can be achieved with other *ab initio* methods[36] and is typical of what *ab initio* theory can provide for assessing density functionals. After completing our CASPT2 study, we decided to also include results from the recently developed SORCI method.[16] This method has some features in common with the CASPT2 method, such as the combination of perturbation theory and multireference methods, but differs markedly in other ways, such as its accent on the calculation of energy differences and its ability to go beyond the limit of about 14 active orbitals frequently found in CASSCF and CASPT2 to as many as 40 or 50 active orbitals. Thus the SOCI method offers an interesting ''second opinion'' for comparison with our CASPT2 work.

1. Programs and basis sets

Our *ab initio* calculations were carried out with three different programs. The program GAUSSIAN was used to carry out spin-restricted Roothaan–Hartree–Fock (i.e., SCF) calculations (as well as some second-order Møller–Plesset calculations which we did not find interesting enough to report here). Our CASSCF and CASPT2 calculations were carried out with the program MOLCAS.[38] Spin-restricted Roothaan–Hartree–Fock (SCF) calculations were also carried out with MOLCAS. Our SOCI calculations were carried out with the ORCA program.[39] All of these programs use basis sets consisting of Gaussian-type orbitals, so that the same basis could (and frequently was) used in calculations using different programs. At the same time, the need for a more or less sophisticated basis set differs from method to method as does the amount of computer resources needed to perform a calculation with a given basis set. The basis sets used in our calculations are summarized in Table I. They will be described in more detail below, in the context of the various methods used.

TABLE I. Summary of basis sets used in this work.

Name	Basis sets			Size
	Fe	O	H	
	Contracted Gaussian-type orbitals			
A	DZVP	DZVP	DZVP	132
A′	6-31G*	6-31G*	6-31G*	142
D	6-31G*	6-31G*	6-31G**	178
F	(8s6p4d2f) Wachters	TZVP Ahlrichs	TZV Ahlrichs	182
B	DZVP CS	6-31G**++	6-31G**	192
C	TZVP Ahlrichs	TZVP Ahlrichs	TZVP Ahlrichs	219
E	6-31G*	6-311G**++	6-311G**++	250
B′	6-31G*	6-311G++(3df,3pd)	6-311G**	340
	Slater-type orbitals			
C″	TZ2P	TZ2P	TZ2P	379

2. CASSCF and CASPT2 calculations

The orbital basis sets used in our MOLCAS calculations were of 6-31G* and 6-31G** quality.[40,41] For the atom, we also used the larger ANO-S basis set.[42] In the CASSCF and CASPT2 calculations, we have employed two different active spaces—namely, CAS1 and CAS2. In the CAS1, the six *d* electrons were distributed among the five *d* orbitals (i.e., CASSCF[6,5] and CASPT2[6,5]). As illustrated in Fig. 1, some of the 3*d* orbital density mixes with *p*-type orbitals on the ligand oxygens. It has been found important to include all of this 3*d* density in the CASSCF by expanding the active space to include not only the highest occupied molecular orbital (HOMO) and lowest unoccupied molecular orbital (LUMO) orbitals but also the lowest three and highest two orbitals in the [6,5] calculations to make a [12,10] calcula-

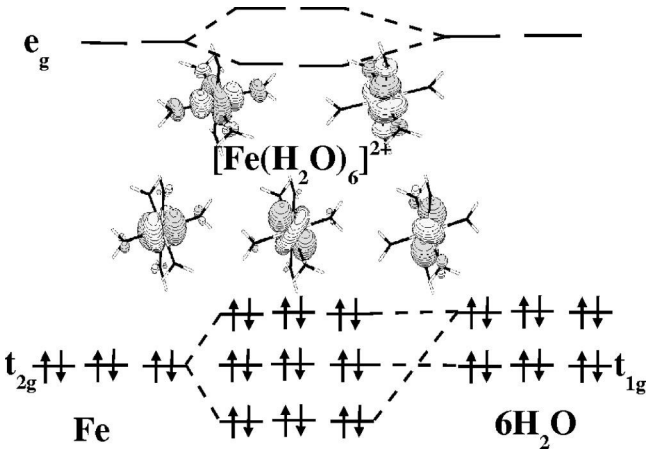

FIG. 1. Correlation diagram for the highest-lying occupied and lowest-lying unoccupied molecular orbitals found in our DFT singlet calculations (not to scale). Also shown are pictures of the HOMOs and LUMOs showing the $d-\pi$ bonding nature of the former and the antibonding nature of the latter. Note that e_g Fe(II) orbitals correlate with e_g $6H_2O$ orbitals and t_{2g} Fe(II) orbitals correlate with t_{2g} $6H_2O$ orbitals, but that there is an absence of t_{1g} Fe(II) orbitals to correlate with the $6H_2O$ orbitals of the same symmetry representation.

tion (i.e., CASSCF[12,10] and CASPT2[12,10]). The strategy of adding this second d shell has been named the "$3d$ double-shell effect."[43–45] It allows a better description of the large radial correlation effects due to the interaction between the $3d$ electrons. Automatic structure optimization and frequency calculations (to confirm minima) were carried out at the CASSCF level. This was not possible at the CASPT2 level where only single-point calculations were performed. In addition, the lowest 30 orbitals were frozen in the molecular CASPT2 calculation.

3. SORCI calculations

In addition to the CASPT2 calculations we have used the recently developed SORCI procedure[16] as implemented in the ORCA package.[39] The orbital basis set used in our SORCI calculations (basis set F in Table I) consists of Wachters basis set for Fe (Ref. 46) supplemented with appropriate f functions (Ref. 47), Ahlrichs TZVP basis set for O (Ref. 48), and Ahrichs TZV basis set for H (Ref. 48). As explained in detail in Ref. 16, the SORCI method is an individually selecting variation and perturbation approach which combines multiconfigurational second-order Møller–Plesset perturbation theory with the difference-dedicated configuration concept of Malrieu co-workers.[14,15] The method introduces three cutoffs to achieve applicability to molecules with up to ~50 atoms or ~700 basis functions. The cutoffs control the reduction of the reference space (T_{pre} chosen to be 10^{-5}), the size of the variational space (T_{Sel} chosen to be $10^{-6}E_h$), and the size of the approximate average natural orbital (AANO) basis (T_{Nat} chosen to be 10^{-4}). The calculations were carried out at the B3LYP-optimized geometries. The orbitals came from a spin-averaged Hartree–Fock (SAHF) calculation according to Zerner.[49,50] In the SAHF method, one obtains orbitals that are optimized for the average of all states of a given multiplicity that can be formed within a configuration of n electrons in m orbitals. In the present case, the SAHF calculation was done for six electrons in the five iron $3d$-based molecular orbitals. This procedures avoids any pitfalls of converging to low-lying excited states and is thought to be an ideal starting point for the following correlated calculations. The initial reference space for the SORCI calculations was CAS(6,5). Since the SORCI method is designed to provide energy differences at fixed geometry, an estimate of the change in total energy in going from the high-spin ($S=2$) to the low-spin ($S=0$) geometry must be provided in order to obtain the adiabatic excitation energy. This number was estimated from DDCI3 (difference-dedicated configuration interaction calculations with choice 3 of screening procedure[15,16]) calculations at the optimized singlet and quintet geometries, respectively, and employed the estimate proposed by Castell *et al.* for the effect of the inactive double excitations.[51] The correction amounts to 807 cm^{-1}, which was added to the vertical quintet–singlet excitation energy calculated at the singlet optimized geometry.

4. SCF convergence

At the SCF level, in both our Hartree–Fock and DFT calculations, convergence to the wrong electronic state was frequently encountered. This problem was overcome by a series of calculations using restart files for different size basis sets. Correct convergence for the LS electronic state was further confirmed by Cancès who was able to reproduce our result with his more robust fractional occupation convergence algorithm.[52]

B. DFT calculations

The DFT calculations reported here were carried out with GAUSSIAN (Ref. 53) and with ADF (Ref. 54). These programs differ in several respects, making comparisons between them ideal for distinguishing numerical artifacts and algorithmic features from differences due to the choice of functional. Among the algorithmic differences, the most important is certainly that GAUSSIAN uses basis sets of Gaussian-type orbitals (GTOs) while ADF uses Slater-type orbital (STO) basis sets. These two types of basis sets behave rather differently and it is difficult to say *a priori* which GTO and STO basis sets should be of comparable quality. The basis sets used in this study are summarized in Table I. In order to be thorough and to verify convergence with respect to the quality of the different basis sets, calculations were carried out with basis sets A, A′, B, B′, C, D, and E. However, we have opted to present only results for basis sets A′, C, and E as these are adequate for illustrating the main points of our discussion. We were unable to converge our ADF calculations for the HS state with the LDA and the C″ basis set.

Atomic DFT calculations. Our *ab initio* calculations use wave functions which belong to correct space and spin representations, which sometimes requires a linear combination of several Slater determinants. In contrast, DFT is based on calculations with single Slater determinants, making the DFT treatment of atomic multiplet states conceptually different in nature than in the *ab initio* calculations. The DFT calculations for the atomic limit [$^5D-{}^1I$ splitting of $Fe^{2+}(d^6)$] reported here have been carried out using the "multiplet-sum method"[55–58] (MSM). In particular, we have followed the MSM procedure for d^n (s^2d^n) atomic multiplets given in Ref. 58. The basic idea of the MSM is described in the Appendix. The MSM calculations reported here were carried out using the ADF program.

IV. RESULTS

This section presents a critical analysis of our *ab initio* and DFT results for the HS and LS states of the hexaquoferrous cation $[Fe(H_2O)_6]^{2+}$. A qualitative understanding of these two states can be obtained from simple LFT considerations, assuming a complex with O_h symmetry. Since water is a low-field ligand, the pair repulsion energy is expected to be more important than is the ligand splitting energy. The ground state is thus expected to be the HS state

$$FeL_6{}^{2+}[{}^5T_{2g}:\ (t_{2g})^4(e_g)^2]\rightarrow Fe^{2+}({}^5D)+6L, \qquad (4.1)$$

while the LS state

$$FeL_6{}^{2+}[{}^1A_{1g}:\ (t_{2g})^6(e_g)^0]\rightarrow Fe^{2+}({}^1I)+6L \qquad (4.2)$$

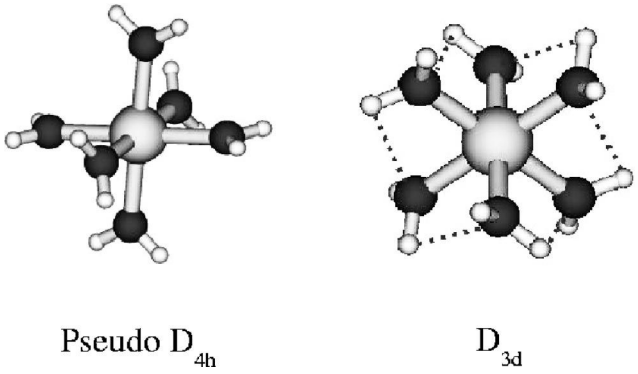

FIG. 2. Two pseudosymmetries found for $[Fe(H_2O)_6]^{2+}$ in our calculations. Arrows have been added to the D_{4h} structure to indicate a Jahn–Teller distortion. Dotted lines have been added to the D_{3d} structure to indicate the presence of weak H-bonding interactions. The distortion of the D_{3d} structure has been exagerated for clarity.

is expected to lie at considerably higher energy (L stands for water). In fact, while the HS state is reasonably well characterized experimentally, almost nothing appears to be known about the LS state.

A. Optimized geometries

We now consider the geometrical structure of the free gas-phase cation. Two main types of geometries have been found and these are shown schematically in Fig. 2. Our results for the HS state are summarized in Tables II and III.

1. Ab initio: HS results

As expected, the CASSCF results are dominated by a single determinant (coefficient=0.990) indicating a lack of strong static correlation contributions and that the independent particle model is a reasonable zero-order starting point for qualitative discussions (note, however, that dynamic correlation is important at a quantitative level and might eventually also lead to changes in the qualitative picture.) According to the simple LFT model [Eq. (4.1)], this electronic state is degenerate in O_h symmetry. We should therefore expect a Jahn–Teller distortion. This distortion appears in the *ab initio* results as a shortening of the two axial Fe–O bonds relative to the four equatorial Fe–O bonds. At the same time, the D_{4h} symmetry complex (neglecting hydrogens) is broken by a slight inclination (1.7°) of the O–Fe–O axis with respect to perpendicularity with the equatorial plane of the molecule. This inclination allows a slight reduction of the O–H distance between a hydrogen of each axial water and an oxygen of each of two opposing equatorial waters. The hydrogen atoms of the other two equatorial waters compensate by rotating about 11.4° out of the equatorial plane.

TABLE II. $^5T_{2g}\,[Fe(H_2O)_6]^{2+}$ bond lengths. Our notation is based upon the idea of a pseudo D_{4h} structure since, neglecting the hydrogens, this is what we find in our best calculations. Footnotes indicate geometries which, neglecting the hydrogens, are better described as D_{3d} and give the OFeO C_{3v} angle.

Method	$^5T_{2g}\,[Fe(H_2O)_6]^{2+}$ Equatorial R(Fe–O) (Å)	Axial R(Fe–O) (Å)
	MOLCAS	
CASSCF(12,10)	2.194	2.171
	GAUSSIAN	
$X\alpha$/A′[a]	2.070	2.070
SVWN/A′[a]	2.056(2)	2.051
BP86/A′	2.134(8)	2.101
BP86/C	2.165(0)	2.130
BP86/E	2.154(6)	2.126
BLYP/C	2.190(4)	2.152
BLYP/E	2.180(2)	2.138
PW91/C	2.160(5)	2.124
PW91/E	2.150(6)	2.112
B3LYP/C	2.174(6)	2.143
B3LYP/E	2.166(1)	2.131
	ADF	
BP86/C″	2.158(4)	2.120
PW91/C″	2.155(5)	2.118
PBE/C″	2.160(0)	2.122
RPBE/C″	2.201(0)	2.160

[a]D_{3d} with a OFeO C_{3v} angle of 101(1)°.

TABLE III. $^5T_{2g}\,[Fe(H_2O)_6]^{2+}$ bond angles. Our notation is based upon the idea of a pseudo-D_{4h} structure since, neglecting the hydrogens, this is what we find in our best calculations. Footnotes indicate geometries which, neglecting the hydrogens, are better described as D_{3d} and give the OFeO C_{3v} angle. The abbreviation NA appears in the table for these entries to indicate that the D_{4h} angles are "not applicable."

Method	$^5T_{2g}\,[Fe(H_2O)_6]^{2+}$ ∠OFeO′	Dihedral OFeO′H
	MOLCAS	
CASSCF(12,10)	91.9	11.4
	GAUSSIAN	
$X\alpha$/A′[a]	NA	NA
SVWN/A′[a]	NA	NA
BP86/A′	90.8	15.5
BP86/C	90.7	15.2
BP86/E	90.9	18.3
BLYP/C	91.0	14.7
BLYP/E	90.9	17.4
PW91/C	90.7	15.1
PW91/E	91.0	17.7
B3LYP/C	91.0	14.1
B3LYP/E	91.3	15.7
	ADF	
BP86/C″	90.6	16.1
PW91/C″	90.6	15.8
PBE/C″	90.7	15.9
RPBE/C″	90.6	15.0

[a]D_{3d} with a OFeO C_{3v} angle of 101(1)°.

2. DFT: HS results

Geometries optimized using the LDA functional have six almost equal Fe–O bond lengths in a D_{3d}-type distortion. In both the exchange-only ($X\alpha$) and exchange-correlation (SVWN) cases, these bond lengths are significantly shorter than the *ab initio* values. A comparison between the $X\alpha$ and SVWN geometries shows that including correlation shortens bond lengths. However, the LDA bond lengths are too short compared with the *ab initio* results. Including gradient corrections via the BP86 functional increases the bond lengths as compared to the LDA. Augmenting the quality of the basis sets leads to further bond length increases and tidies up the geometry so that it is no longer a D_{3d}-type structure, but is

TABLE IV. Experimental $[Fe(H_2O)_6]^{2+}$ geometries. Bond distances in Å, bond angles in degrees.

$[Fe(H_2O)_6]^{2+}$			
R(FeO)	R(OH)	∠HOH	∠OFeO′
	Fe(II) salts in solution[a]		
2.114			
	Fe(II) salts in solution[b]		
2.095			
	Fe(II) salts in solution[c]		
2.12			
	Fe(II) salts in crystal[d]		
2.13			
	$FeSiF_6 \cdot 6H_2O$[e]		
2.146	0.924	111.9	91.4
	0.920		88.6
	$FeSO_4 \cdot 7H_2O$[f]		
2.068			90.5
2.144			92.9
2.136			94.0
	$FeSO_4 \cdot 7H_2O$[g]		
2.096			90.5
2.109			91.0
2.188			92.4
	$Fe(NH_4)_2(SO_4)_2 \cdot 6H_2O$[h]		
2.156			89.3
2.136			90.9
2.086			91.2
	$[TMA]_2[Fe(H_2O)_6]Mo_8O_{26}$[i]		
2.11			
2.10			

[a]Average values from different x-ray and extended x-ray-absorption fine-structure (EXAFS) studies (Ref. 63).
[b]From EXAFS data (Ref. 64).
[c]From x-ray data (Ref. 64).
[d]Average value originating from different x-ray studies (Ref. 64).
[e]Neutron scattering crystal data (Ref. 65). The two angles correspond to the two different angles of a D_{3d} structure.
[f]Melanterite, parameters from site 1 in the crystal which was found to have two different D_{2h} sites (Ref. 66). An OH bond distance of 0.97 Å and an HOH angle of 109.5° was assumed by the author.
[g]Melanterite, parameters from site 2 in the crystal which was found to have two different D_{2h} sites (Ref. 66). An OH bond distance of 0.97 Å and an HOH angle of 109.5° was assumed by the author.
[h]Ammonium Tuton salt (Ref. 67).
[i]X-ray crystal data (Ref. 68). The $[Fe(OH_2)_6]^{2+}$ octahedron is stretched along the threefold axis. Two slightly different OH distances are reported for the water molecules. Authors indicate that all reported values, except bond angles, have been corrected for thermal motion.

now the same D_{4h} pseudosymmetry as the CASSCF results, but with a smaller inclination of the equatorial waters and a larger angle of rotation out of the plane.

As might be expected, we were unable to find any experimental structural data for the free gas-phase cation, but a large amount of solution and crystallographic data exists for this cation in conjunction with various anions. These data has been collected in Table IV. The observed bond lengths are in the range 2.07–2.19 Å in agreement with both the *ab initio* and DFT calculations with GGA and hybrid functionals. Apparently, depending upon the salt considered, either the axial waters have moved *out* and the equatorial waters have moved *in* ($FeSO_4 \cdot 7H_2O$) or the axial waters have moved *in* and the equatorial waters have moved *out* $[Fe(NH_4)_2(SO_4)_2 \cdot 6H_2O]$ in agreement with the results of both the *ab initio* and DFT calculations. Given the very small difference (~0.04 Å) between the calculated equatorial and axial Fe–O bond lengths, we conclude from the results of the *ab initio* and DFT calculations that the Jahn–Teller effect is rather weak. Consequently, the more pronounced differences in the Fe–O bond lengths seen in the experimental geometries in Table IV should be interpretted as indicating that crystal packing effects are strong and dominate the much weaker Jahn–Teller effect.

3. LS: Ab initio and DFT results

Our results for the LS state are summarized in Table V. According to the simple LFT model [Eq. (4.2)], this electronic state is nondegenerate in the O_h symmetry and no Jahn–Teller distortion is expected. This is what is found in our *ab initio* calculations. The bonds are distinctly shorter in the LS state than in the HS state, consistant with the idea that the e_g orbital occupied in the HS state is antibonding in nature. The DFT calculations also show a single Fe–O bond length, but show a slight distortion to the pseudo-D_{3d} structure, apparently because this allows energetically favorable H-bonding interactions (see Fig. 2). It should be emphasized, however, that this apparent H-bonding interaction is highly unlikely to be real and gradually disappears as the calcula-

TABLE V. $^1A_{1g}\,[Fe(H_2O)_6]^{2+}$ geometry. A D_{3d} geometry has been assumed, neglecting hydrogens. The OFeO angle given is between oxygens related by the C_{3v} symmetry operation. The complex geometry becomes O_h when this angle is 90°.

Method	$^1A_{1g}\,[Fe(H_2O)_6]^{2+}$ R(Fe–O) (Å)	∠O–Fe–O (°)
	MOLCAS	
CASSCF(12,10)	2.077	90.0
	GAUSSIAN	
$X\alpha$/A′	1.917	96.9(1)
SVWN/A′	1.912	98.7(1)
BP86/A′	1.985	96.2(2)
BP86/C	2.018	94.5
BP86/E	1.996	90.0
BLYP/C	2.045	93.7
BLYP/E	2.025	90.0
PW91/A′	1.980	95.5(1)
PW91/C	2.014	94.5
PW91/E	1.992	90.0
B3LYP/A′	2.010	96.2(2)
B3LYP/C	2.032	90.0
B3LYP/E	2.018	90.0
	ADF	
BP86/C″	2.010	94.3
PW91/C″	2.007	94.3
PBE/C″	2.011	94.4
RPBE/C″	2.048	94.2

tions become more realistic. Adding electron correlation at the local level ($X\alpha \rightarrow$SVWN) reduces this distortion. Both gradient corrections and extending the basis set initially enhance the distortion and then, with the largest basis set (E), bring the structure back to O_h symmetry. However, it is worth emphasizing that the distortion of the D_{3d} from the O_h structure is almost always relatively small as emphasized by the superposition of the BP86/B′ HS and LS structures shown in Fig. 3. The comparison between the geometries of HS and LS states shows that, on average, the Fe–O bond lengths are ~0.15 Å longer in the HS state. This difference $\Delta R_{HL}=R_{HS}-R_{LS}$ takes here a value which is slightly less than the value of ~0.2 Å expected for spin-crossover compounds with a $[FeN_6]$ coordination sphere.[59] This difference may be attributed to the π-backbonding effects which take place in spin-crossover $[FeN_6]$ compounds (for which a common feature is the use of π ligands) and are responsable for their t_{2g} orbitals being more bonding than in the case of the hexaquoferous cation.

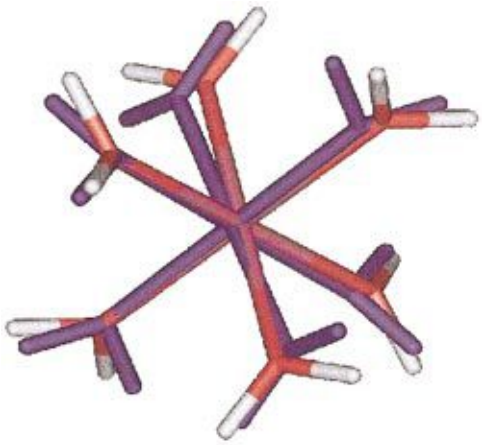

FIG. 3. (Color) Superposition of the LS (single color) and HS (multicolor) $[Fe(H_2O)_6]^{2+}$ minima found at the BP86/B′ level of calculation.

TABLE VI. Comparison of atomic excitation energies.

Method	Fe^{2+} excitation energy: $^5D\rightarrow{}^1I$ Energy (cm^{-1})	Energy (eV)
Expt.[a]	29897.3	3.70
	ab initio	
CI[b]	33800.0	4.19
CASSCF(6,10)/6-31G*	33185.0	4.11
CASSCF(6,10)/ANO-S	32850.0	4.07
CASPT2(6,10)/6-31G*	33735.0	4.18
CASPT2(6,10)/ANO-S	32130.0	3.98
DDCI3	33200.0	4.12
	DFT ADF	
SVWN/TZ2P	29988.0	3.59
BP86/TZ2P	30529.0	3.79
PW91/TZ2P	29845.0	3.70
PBE/TZ2P	30321.0	3.76
RPBE/TZ2P	30238.0	3.75

[a] $^5D\rightarrow{}^1I$ transition from National Institute of Science and Technology (NIST) Atomic Spectra Database (http://physics.nist.gov/cgi-bin/AtData/main_asd). See text.
[b]Reference 60.

B. Energetics

The HS–LS energy difference is a far more sensitive test of the quality of a density functional than is the structure.

1. Atomic limit

We first consider the atomic limit. Results are collected in Table VI.

A few remarks are in order regarding the "experimental" $^5D\rightarrow{}^1I$ Fe^{2+} excitation energy. The number given in Table VI is derived from the observation that the experimental transition energies given in the National Institute of Science and Technology (NIST) Atomic Spectra Database are well described by the Russell–Saunders coupling scheme and the formula

$$E_{SO}(^{2S+1}L_J)=\tfrac{1}{2}A[J(J+1)-L(L+1)-S(S+1)] \qquad (4.3)$$

for the spin–orbit energy, where A depends on L and S, but not on J (see, for example, p. 336 of Ref. 35). Since

$$\frac{\sum_{J=|L-S|}^{L+S}(2J+1)E_{SO}(^{2S+1}L_J)}{\sum_{J=|L-S|}^{L+S}(2J+1)}=0, \qquad (4.4)$$

we remove spin–orbit coupling from the experimental multiplet energies by a simple degeneracy-weighted average:

$$\bar{E}(^{2S+1}L)=\frac{\sum_{J=|L-S|}^{L+S}(2J+1)E(^{2S+1}L_J)}{\sum_{J=|L-S|}^{L+S}(2J+1)}. \qquad (4.5)$$

This analysis shows the magnitude of spin–orbit coupling ($A \approx 100\,\mathrm{cm}^{-1}$) and provides the experimentally derived $[\bar{E}(^1I) - \bar{E}(^5D)]$ spin–orbit-free excitation energy in Table VI. Had we instead used the observation that

$$E_{\mathrm{SO}}(^5D_3) = 0, \tag{4.6}$$

the resultant spin–orbit-free ^5D energy would only differ from the degeneracy-weighted multiplet energy average by about 23 cm^{-1}.

The best available *ab initio* calculation overestimates the excitation energy by about 1800 cm^{-1}. To keep this in perspective, 350 cm^{-1} (1 kcal/mol or "chemical accuracy") is an often cited, but difficult to achieve, objective for quantum chemical methods, while 1749 cm^{-1} (5 kcal/mol) is more typical of what can be obtained from the best *ab initio* and DFT methods. In this case, the error is on the high end of what is expected, but reasonable. However, this is only with the relatively large ANO-S basis set, which is too large to apply in *ab initio* calculations on the full complex. This is why atomic information is used to empirically correct the molecular HS–LS energy difference,[60] particularly when basis set saturation becomes impossible.

The DFT results reported in Table VI were calculating using the multiplet-sum method described in the Appendix. This method has not been used in any of our molecular calculations, but is needed in the atomic case because of the essential multideterminantal nature of the atomic multiplets. The multiplet-sum method is not a formally exact method, but is known to provide useful first-order estimates of excitation energies. As we have seen, the $^5D \rightarrow {}^1I$ transition in Fe^{2+} poses problems for high-quality *ab initio* methods. Our expectations regarding the quality of first-order DFT estimates of this quantity should be moderate at best. Nevertheless, the results in Table VI show that the multiplet-sum method implemented in the ADF program gives excellent results. With the best basis (TZ2P) the LDA (VWN) gives an excitation energy which is only 368 cm^{-1} too low compared to experiment. Similar or smaller errors are found with GGA functionals and the same basis set: 173 cm^{-1} for the BP86, 511 cm^{-1} for the PW91, 352 cm^{-1} for the PBE, and 118 cm^{-1} for the RPBE functionals. Thus there appears to be no justification in DFT for an atom-based empirical correction for the molecular HS–LS energy difference.

2. Molecular energy differences

Calculated HS–LS energy differences for the hexaquo complex are shown in Table VII for the molecular case. The importance of electron correlation is immediately seen in the case of the *ab initio* calculations. Inclusion of higher levels of correlation decreases the HS–LS energy difference, indicating that electron correlation is more important for the higher-lying (LS) than for the lower-lying (HS) state. Our CASSCF[6,5] results are in good agreement with those previously reported by Åkeson *et al.*[60] However, increasing the active space to include the $3d$ double-shell effect further decreases the HS–LS energy difference. Our CASPT2[12,10] calculations (which include the $3d$ double-shell effect) are in good agreement with the CI energy difference reported by Åkeson *et al.*, who noted that a better estimate of the true HS–LS energy difference might be obtained by using the difference between calculated and atomic excitation energies to correct the molecular HS–LS energy difference:

TABLE VII. $[Fe(H_2O)_6]^{2+}$ LS–HS energy differences as calculated directly and after shifting the asymptotes of the dissociation curves to match the known experimental atomic $Fe^{2+}\ {}^5D \rightarrow {}^1I$ energy difference.

	LS–HS energy differences (cm^{-1})	
Method	Direct	Shifted[a]
SCF[b]	27500.0	
CASSCF[b]	23200.0	
CI[b]	17100.0	13700.0
CASSCF(6,5)/D	23125.0	
CASSCF(12,10)/D	21180.0	17892.0
CASPT2(6,5)/D	21610.0	
CASPT2(12,10)/D	16185.0	12347.0
SORCI	13360.0	
	GAUSSIAN	
$X\alpha$/A′	11273.0	
SVWN/A′	2745.0	
BP86/A′	9069.0	
BP86/C	8505.0	
BP86/E	9374.0	
BLYP/C	8388.0	
BLYP/E	9084.0	
PW91/C	8959.0	
PW91/E	9761.0	
B3LYP/C	11456.0	
B3LYP/E	11783.0	
	ADF	
BP86/C″	8696.0	
PW91/C″	8225.0	
PBE/C″	9056.0	
RPBE/C″	11844.0	

[a]CI atomic correction from Ref. 60. Other atomic corrections calculated from data in Table VI.
[b]Reference 60.

$$\Delta E_{LH}^{\mathrm{shifted}} = \Delta E_{LH}^{\mathrm{direct}} + (\Delta E_{\mathrm{atom}}^{\mathrm{expt}} - \Delta E_{\mathrm{atom}}^{\mathrm{calc}}). \tag{4.7}$$

This shift makes sense if part of the molecular error is inherited from the error in the asymptotic energies of the dissociated complex ($Fe^{2+}\ {}^5D$ or $^1I + 6\ H_2O$ ground-state energies). This shift further lowers the best *ab initio* values for the HS–LS energy difference by about 3000 cm^{-1} to give a best estimate of the true HS–LS energy difference in the range

$$12\,000\ \mathrm{cm}^{-1} < \Delta E_{LH}^{\mathrm{best}} < 13\,000\ \mathrm{cm}^{-1}. \tag{4.8}$$

At the singlet-optimized geometry, the SORCI calculations provide a $^1A_{1g}$ vertical excitation energy of 12 553 cm^{-1}. Accounting for the geometric relaxation which stabilizes the quintet state by another 807 cm^{-1}, we arrive at an adiabatic excitation of

$$\Delta E_{LH}^{\mathrm{direct}} = 13\,300\ \mathrm{cm}^{-1} \tag{4.9}$$

without any empirical shift. This number is in agreement with the best estimate from the CASPT2 calculations. It is rationalized by the generally good success of the SORCI method for d–d spectra[61] which accounts for the high-order effects of the most strongly perturbing configuration-state

functions in the outer space. We therefore believe the uncorrected SORCI HS–LS energy difference.

Adding correlation (SVWN) to exchange-only ($X\alpha$) LDA calculations also results in a decrease in the value of the HS–LS energy difference. The amount of the decrease is comparable to that seen at the *ab initio* level (about 10 000 cm^{-1}), but the final LDA value of about 3000 cm^{-1} is far too small. This is certainly in line with the idea that the LDA underestimates Fermi correlation and so gives too low a quintet energy relative to the singlet energy.

Going to GGAs increases the value of the HS–LS energy difference by about 3000 cm^{-1} and improving the basis set leads to another increase of about 3000 cm^{-1}. The final result varies between about 7500 and 9500 cm^{-1}, which, while in significantly better agreement with our best estimate of the true HS–LS energy difference than is the LDA value, is still too low by a few thousand wave numbers. An exception is the RPBE functional, which gives a HS–LS energy difference of about 12 000 cm^{-1}, in remarkable agreement with the *ab initio* best estimate.

The hybrid functional B3LYP gives a HS–LS energy difference of about 11 500 cm^{-1}, similar to the RPBE value, but not as close to the *ab initio* best estimate. It certainly would be interesting to see how the multiplet-sum method would work for energies excitation with the B3LYP functional; however, we were not able to perform multiplet-sum atomic calculations with this functional due to the software limitations.

Since we have the HS–LS energy difference for both the B3LYP and BLYP functionals and the HS–LS energy difference is to a good approximation linear in the a_0 exchange-mixing parameter, we can also estimate the value of the HS–LS energy difference with the B3LYP* functional: 8500 cm^{-1} with basis A, 9700 cm^{-1} with basis B, 10 689 cm^{-1} with basis C, 10 800 cm^{-1} with basis D, and 11 100 cm^{-1} with basis E. In this case the B3LYP* functional appears to correct the B3LYP HS–LS energy difference in the wrong direction compared to the *ab initio* best estimate. However, it should be kept in mind that the RPBE, B3LYP, and B3LYP* results are all very close to our *ab initio* best estimates for the HS–LS energy difference.

C. Comparison of STO- and GTO-based DFT calculations

As mentioned in Sec. III, it is difficult to say *a priori* which GTO and STO basis sets should be of comparable quality. This is especially true because GTO and STO basis sets have qualitative differences that can lead to systematic errors which cancel when taking differences. However, as shown in Table VIII we can say *a posteriori* that ADF calculations with the C″ basis set (TZ2P) give energies and geometries similar to those obtained in GAUSSIAN calculations with the C basis set (Ahlrichs TZVP) for DFT calculations with the BP86 and PW91 functionals. In retrospect, this seems reasonable since the two basis sets have roughly the same degree of flexiblity. Note, however, that the we have more confidence in results obtained with the E basis set since the E basis set is more flexible than is the C basis set. In order to be able to compare results obtained with functionals available only in ADF with the results of functionals only available in GAUSSIAN, the ADF C″ results have been scaled to make the "E" basis set results in Table VIII. Results with the E and "E" basis sets have been used to prepare Fig. 4, which provides a nice summary of the principal results of this paper.

TABLE VIII. Calculated bond length and energy differences between high- and low-state structures for selected basis sets and functionals. The results for basis set "E" were obtained by multiplying the ΔR_{HL} results for basis set C″ by 1.08 and the ΔE_{LH} results for basis set C″ by 1.07.

Method	$[Fe(H_2O)_6]^{2+}$ ΔR_{HL} (Å)[a]	ΔE_{LH} (cm^{-1})[b]
	ADF	
BP86/C″	0.130	9255
PW91/C″	0.130	9250
PBE/C″	0.136	9256
RPBE/C″	0.139	11844
BP86/"E"	0.140	9903
PW91/"E"	0.140	9898
PBE/"E"	0.147	9904
RPBE/"E"	0.150	12673
	GAUSSIAN	
BP86/C	0.135	8505
PW91/C	0.130	8959
BLYP/C	0.132	8388
B3LYP/C	0.132	11456
BP86/E	0.149	9374
PW91/E	0.145	9761
BLYP/E	0.141	9084
B3LYP/E	0.136	11783

[a] $\Delta R_{HL}=R_{LS}-R_{HS}$ where R refers to the weighted average of the Fe–O bond distances (i.e., 4 times the equitorial Fe–O distance plus 2 times the axial Fe–O distance, and the whole quantity divided by 6).
[b] $\Delta E_{LH}=E_{LS}-E_{HS}$.

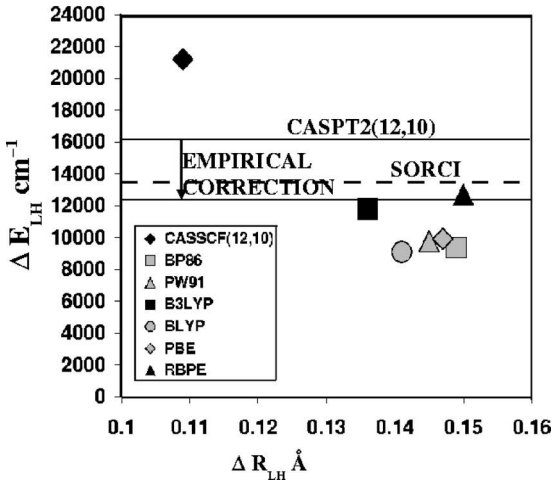

FIG. 4. Comparison of *ab initio* and DFT best estimates for bond length and energy differences between the high- and low-spin states of $[Fe(H_2O)_6]^{2+}$. Results of atomic calculations have been used to empirically correct our CASPT2(12,10) energy difference for an insufficiently large basis set. DFT results are for GAUSSIAN calculations with the E basis set and ADF calculations with the fictious "E" basis set. (PW91 results shown only for the GAUSSIAN calculations.) In particular, ADF results with the C″ basis set have been empirically scaled in order to estimate what they would be with the better E basis set. See text for further details.

V. CONCLUSION

It is now possible to carry out rigorous *ab initio* and density-functional theory calculations on transition-metal complexes and, while the former tend to be limited to simpler complexes, the latter can be applied to molecules of practical interest. Neither method is expected to replace ligand field theory anytime in the near future. Indeed, LFT provides an excellent starting point for beginning to understand the electronic properties of transition-metal complexes and can even provide better numerical values than either *ab initio* or DFT when properly parametrized for specific properties of interest. However, LFT has important limitations, especially when considering changes in geometry and the consequent changes in ligand field strengths, and this is where the more rigorous models are expected to make important contributions. These aspects play a crucial role in understanding the light-induced excited-state spin trapping phenomenon in Fe(II) compounds, and so we may expect *ab initio* and especially (because of the size of the molecules involved) DFT to make an important contribution to modeling LIESST. Unfortunately, relatively little is known about the intrinsic applicability of these more rigorous models to Fe(II) coordination complexes. This paper presents a first study concerning the accuracy and choice of density functionals in the context of the simple "textbook" complex $[Fe(H_2O)_6]^{2+}$. Little experimental data are available for these complexes, though x-ray crystal structures are available for compounds containing the high-spin cation. However, we have compensated for this by performing *ab initio* calculations at the CASPT2 and SOCI levels with reasonably extensive basis sets.

It should be noted that the CASPT2 calculations are far from being a "black box" because of the question of how to choose the active space in the multiconfigurational calculations. In principle, this is one of the reasons that DFT is often preferred over *ab initio* methods for treating transition-metal complexes. However, we have found that this is somewhat countered by the tendency of DFT to converge to the incorrect electronic state unless great care is taken to analyze results for possible excited states and treat them accordingly. This is certainly one reason why some workers prefer multiconfigurational calculations to DFT calculations for these compounds. However, multiconfigurational calculations soon become unmanageable as the compounds become large (at least if the active space is also increased) and so we have concentrated on developing tricks to help guarantee convergence of DFT to the right electronic state. Our most useful tool has turned out to be the clever use of sequences of restart files to guide our calculations, combined with careful examination of the molecular orbitals. Ultimately, however, we think that the algorithm of Cancès will be helpful in mitigating this problem.[52]

Both our *ab initio* and DFT optimized geometries are consistant with the available experimental data. More importantly (given the relative lack of detailed experimental data), our DFT geometries are found to be consistent with our *ab initio* geometries provided functionals are used which go beyond the local level and large basis sets are used. Of course, our objective here has been to test functionals by focusing on details, but it should be kept in mind that smaller basis sets may be adequate for many practical applications.

The low-spin–high-spin energy difference ΔE_{LH} is a far greater challenge for theory. Here there are no available experimental data for $[Fe(H_2O)_6]^{2+}$, but there are for the atom. Our CASPT2 calculations are consistent with previous *ab initio* work[62] indicating that there is a systematic overestimation of the difference of the atomic asymptotes of about 3000 cm^{-1}. When this correction is added to our molecular calculations, we obtain a best estimate of the ΔE_{LH} in the range of about 12 000–13 000 cm^{-1}. The SOCI method gives the same best estimate of ΔE_{LH} *without the need for a semiempirical correction*. In striking contrast, the values of ΔE_{LH} obtained from DFT show wide variations depending upon the class of functional, with about 3000 cm^{-1} with the local functional, about 8000–10 000 cm^{-1} for better basis sets and GGAs other than the RPBE functional and about 12 000 cm^{-1} for the B3LYP hybrid and RPBE GGA functionals. An estimate of what ΔE_{LH} would be for the B3LYP* functional suggests that this is one case where reducing the exact exchange contribution to the B3LYP functional may not be a good idea, although one should be hesitant about overinterpreting this conclusion since it is based on an *ab initio* best estimate which itself is not entirely certain.

It is important to realize that, while the B3LYP and RPBE values of ΔE_{LH} look very good compared with the best estimate available from *ab initio* calculations, all DFT results very much underestimate the *uncorrected* ΔE_{LH} *ab initio* value of about 16 000–17 000 cm^{-1}. That is, it is not enough to examine DFT for the molecule; we must also look at the atomic asymptotes. We were able to do this for local and GGA functionals using the multiplet-sum method (though not for the B3LYP functional for technical reasons). The results of the multiplet-sum method suggest that no empirical correction is necessary for DFT as was the case for the *ab initio* calculations.

These results are consistant with the idea that the B3LYP and RPBE functionals are the most reliable for our intended application of the various functionals tried. Of course, the present work is a study of only a few aspects of a single molecule, though it is a detailed study. We intend to extend this study in the near future to other aspects of this Fe(II) complex and to other small Fe(II) complexes, providing what we hope will be an excellent data bank for determining the strengths and limitations of DFT for studies of general Fe(II) complexes.

ACKNOWLEDGMENTS

This study was carried out in the context of the *groupe de recherche en Commutateurs Optiques Moléculaires à l'Etat Solide* (COMES). A.F. would like to thank the French *Ministère d'Education* for a *Bourse de Mobilité*. M.E.C. and A.F. would like to thank Pierre Vatton and Denis Charapoff for technical support of the LEDSS and *Center d'Expérimentation pour le Calcul Intensif en Chimie* (CECIC) computers used for many of the calculations reported here and would also like to acknowledge supercomputer time at the *Institut du Développment et des Ressources en Informatique Scientifique* (IDRIS) in the context of IDRIS

Project No. 021576. A.H. and L.M.L.D. acknowledge supercomputer time at the *Centro Svizzero di Calcolo Scientifico* (CSCS) in the framework of the CSCS project entitled "Photophysics and Photochemistry of Transition Metal Compounds: Theoretical Approaches." F.N. acknowledges financial support from the Deutsche Forschungsgemeinschaft in the framework of the priority program "Molecular Magnetism." Dr. Eric Cancès of the *Center d'Enseignement et de Recherche en Mathématiques, Informatique, et Calcul Scientifique* (CERMICS) at the *Ecole National des Ponts et Chaussées* is thanked for his calculations confirming our SCF energies. Dr. Emilia Sicilia and Dr. Nino Russo of the Department of Chemistry at the Università della Callabria (Cozenza, Italy) are thanked for providing us with their optimized basis set (designated as DZVP CS in this article). We would also like to thank Trond Saue, John Perdew, Markus Reiher, and Jeremy Harvey for useful discussions concerning and/or comments on our work.

APPENDIX: MULTIPLET-SUM METHOD

The basic idea of the multiplet-sum method is that DFT should provide a good description of states which are well described by single-determinantal wave functions. Then, since it is well known that atomic multiplet energies can often be expressed to first order as weighted linear combinations of the energies corresponding to single-determinant states, it suffices to find appropriate linear combinations, taking care to eliminate integrals which should be equivalent by symmetry. In the present case, the energy of the atomic multiplet states is expressed as a linear combination of only three nonredundant single determinant energies—namely, as

$$E[^5D] = -2.1000E[\Phi_1] + 0.4333E[\Phi_2] + 2.6667E[\Phi_3], \tag{A1}$$

$$E[^1I] = -0.3000E[\Phi_1] + 0.6333E[\Phi_2] + 0.6667E[\Phi_3], \tag{A2}$$

where

$$\Phi_1 = |\bar{d}_{x^2-y^2} d_{x^2-y^2} d_{z^2} \bar{d}_{z^2} \bar{d}_{xz} d_{xz}|, \tag{A3}$$

$$\Phi_2 = |d_{yz} \bar{d}_{yz} \bar{d}_{x^2-y^2} d_{x^2-y^2} \bar{d}_{xz} d_{xz}|, \tag{A4}$$

$$\Phi_3 = |\bar{d}_{xy} \bar{d}_{yz} \bar{d}_{x^2-y^2} d_{x^2-y^2} \bar{d}_{xz} d_{xz}|, \tag{A5}$$

and overbars indicate spin-β orbitals.

[1] B. N. Figgis and M. A. Hitchman, *Ligand Field Theory and Its Applications* (Wiley-VCH, New York, 2000).
[2] P. Gütlich, A. Hauser, and H. Spiering, Angew. Chem., Int. Ed. Engl. **33**, 2024 (1994).
[3] J. A. Real, E. Andrés, M. C. Muñoz, M. Julve, T. Granier, A. Bousseksou, and F. Varret, Science **268**, 265 (1995).
[4] W. W. Gibbs, Sci. Am. **273**, 22 (1995).
[5] Y. Ogawa, S. Koshihara, K. Koshino, T. Ogawa, C. Urano, and H. Takagi, Phys. Rev. Lett. **84**, 3181 (2000).
[6] H. Paulsen, L. Duelund, H. Winkler, H. Toftlund, and A. X. Trautwein, Inorg. Chem. **40**, 2201 (2001).
[7] M. Reiher, O. Salomon, and B. A. Hess, Theor. Chem. Acc. **107**, 48 (2001).
[8] H. Paulsen, H. Grünsteudel, W. Meyer-Klaucke, M. Gerdan, H. F. Grünsteudel, A. I. Chumakov, R. Rüffer, H. Winkler, H. Toftlund, and A. X. Trautwein, Eur. Phys. J. B **23**, 463 (2001).
[9] O. Salomon, M. Reiher, and B. A. Hess, J. Chem. Phys. **117**, 4729 (2002).
[10] M. Reiher, Inorg. Chem. **41**, 6928 (2002).
[11] G. Baranović, Chem. Phys. Lett. **269**, 668 (2003).
[12] C. W. Bauschlicher, Jr., in *Modern Electronic Structure Theory*, edited by D. R. Yarkong (World Scientific, Singapore, 1995), Pt. II.
[13] P. E. M. Siegbahn, Adv. Chem. Phys. **93**, 333 (1996).
[14] J. Miralles, J. P. Daudey, and R. Caballol, Chem. Phys. Lett. **198**, 555 (1992).
[15] J. Miralles, O. Castell, R. Caballol, and J.-P. Malrieu, Chem. Phys. **172**, 33 (1993).
[16] F. Neese, J. Chem. Phys. **119**, 9428 (2003).
[17] D. Harris, G. H. Loew, and A. Kormornicki, J. Phys. Chem. A **101**, 3959 (1997).
[18] R. G. Parr and W. Yang, *Density-Functional Theory of Atoms and Molecules* (Oxford University Press, New York, 1989).
[19] R. M. Dreizler and E. K. U. Gross, *Density Functional Theory, An Approach to the Quantum Many-Body Problem* (Springer-Verlag, New York, 1990).
[20] W. Koch and M. C. Holthausen, *A Chemist's Guide to Density Functional Theory* (Wiley-VCH, New York, 2000).
[21] W. Kohn and L. J. Sham, Phys. Rev. **140**, A1133 (1965).
[22] S. H. Vosko, L. Wilk, and M. Nusair, Can. J. Phys. **58**, 1200 (1980).
[23] D. C. Langreth and J. P. Perdew, Phys. Rev. B **21**, 5469 (1980).
[24] A. D. Becke, Phys. Rev. A **38**, 3098 (1988).
[25] J. P. Perdew, Phys. Rev. B **33**, 8822 (1986).
[26] C. Lee, W. Yang, and R. G. Parr, Phys. Rev. B **37**, 785 (1988).
[27] J. P. Perdew, J. A. Chevary, S. H. Vosko, K. A. Jackson, M. R. Pederson, D. J. Singh, and C. Fiolhais, Phys. Rev. B **46**, 6671 (1992); **48**, 4978(E) (1993); J. P. Perdew, K. Burke, and Y. Wang, *ibid.* **54**, 16 533 (1996); **57**, 14 999(E) (1998).
[28] J. P. Perdew, K. Burke, and M. Ernzerhof, Phys. Rev. Lett. **77**, 3865 (1996); **78**, 1396(E) (1997).
[29] B. Hammer, L. B. Hansen, and J. Nørskov, Phys. Rev. B **59**, 7413 (1999).
[30] A. D. Becke, J. Chem. Phys. **98**, 1372 (1993).
[31] J. Harris and R. O. Jones, J. Phys. F: Met. Phys. **4**, 1170 (1974).
[32] J. P. Perdew, M. Ernzerhof, and K. Burke, J. Chem. Phys. **105**, 9982 (1996).
[33] Gaussian NEWS **5**(2), 2 (1994).
[34] J. Neugebauer and B. A. Hess, J. Chem. Phys. **118**, 7215 (2003).
[35] I. N. Levine, *Quantum Chemistry*, 5th ed. (Prentice Hall, Upper Saddle River, NJ, 2000).
[36] C. Daniel, Coord. Chem. Rev. **238–239**, 143 (2003).
[37] B. R. Roos, in *New Challenges in Computational Quantum Chemistry*, edited by R. Broer, P. J. C. Aerts, and P. S. Bagus (Department of Chemical Physics and Material Science Centre, University of Groningen, Groningen, The Netherlands, 1994), p. 12.
[38] K. Andersson, M. Barysz, A. Bernhardsson *et al.*, MOLCAS, version 5, Lund University, Sweden (2000).
[39] F. Neese, ORCA—an *ab initio*, density-functional and semiempirical program package, version 2.2, revision 74, 2003 (Max Planck Institut für Bioanorganische Chemie, Mülheim, 2003).
[40] P. C. Hariharan and J. A. Pople, Theor. Chim. Acta **28**, 213 (1973).
[41] V. Rassolov, J. A. Pople, M. Ratner, and T. L. Windus, J. Chem. Phys. **109**, 1223 (1998).
[42] R. Pou-Amerigo, M. Merchan, I. Nebot-Gil, P. O. Widmark, and B. Roos, Theor. Chim. Acta **92**, 149 (1995).
[43] C. Froese-Fischer, J. Phys. B **10**, 1241 (1977).
[44] T. H. Dunning, Jr., B. H. Botch, and J. F. Harrisson, J. Chem. Phys. **72**, 3419 (1980).
[45] B. H. Botch, T. H. Dunning, Jr., and J. F. Harrisson, J. Chem. Phys. **75**, 3466 (1981).
[46] A. J. H. Wachters, J. Chem. Phys. **52**, 1033 (1970).
[47] C. W. Bauschlicher, Jr., S. R. Langhoff, and L. A. Barnes, J. Chem. Phys. **91**, 2399 (1989).
[48] A. Schäfer, C. Huber, and R. Ahlrichs, J. Chem. Phys. **100**, 5829 (1994).
[49] M. C. Zerner, Int. J. Quantum Chem. **35**, 567 (1989).
[50] K. K. Stavrev and M. C. Zerner, Int. J. Quantum Chem. **65**, 877 (1997).
[51] O. Castell, V. M. Garcia, C. Bo, and R. Caballol, J. Comput. Chem. **17**, 42 (1996).
[52] E. Cancès, J. Chem. Phys. **114**, 10 616 (2001).
[53] M. J. Frisch, G. W. Trucks, H. B. Schlegel *et al.*, GAUSSIAN 98, Revision A.7, Gaussian Inc., Pittsburgh, PA, 1998.
[54] Amsterdam Density Functional (ADF) program, Theoretical Chemistry, Vrije Universiteit, Amsterdam, the Netherlands, http://www.scm.com
[55] T. Ziegler, A. Rauk, and E. J. Baerends, Theor. Chim. Acta **43**, 261 (1977).

[56] C. Daul, Int. J. Quantum Chem. **52**, 867 (1994).
[57] C. A. Daul, K. G. Doclo, and A. C. Stückel, in *Recent Advances in Density Functional Methods*, edited by D. P. Chong (World Scientific, Singapore, 1997), Pt. II, p. 61.
[58] T. Mineva, A. Goursot, and C. Daul, Chem. Phys. Lett. **350**, 147 (2001).
[59] A. Hauser, in *Topics in Current Chemistry*, Vol. 233, edited by P. Gütlich and H. A. Goodwin (Springer-Verlag, Heidelberg, in press). See also A. Hauser, in *Topics in Current Chemistry*, Vol. 234, edited by P. Gutlich and H. A. Goodwin (Springer-Verlag, Heidelberg, in press).
[60] R. Åkesson, L. G. M. Pettersson, M. Sandström, and U. Wahlgren, J. Am. Chem. Soc. **116**, 8691 (1994).
[61] F. Neese and G. Olbrich (unpublished).
[62] R. Åkesson, L. G. M. Pettersson, M. Sandström, and U. Wahlgren, J. Am. Chem. Soc. **116**, 8713 (1994).
[63] Y. Marcus, Chem. Rev. (Washington, D.C.) **88**, 1475 (1988).
[64] T. K. Sham, J. B. Hastings, and M. L. Perlman, J. Am. Chem. Soc. **102**, 5904 (1980).
[65] W. C. Hamilton, Acta Crystallogr. **15**, 353 (1962).
[66] W. H. Baur, Acta Crystallogr. **17**, 1167 (1964).
[67] H. Montgomery, R. V. Chastain, J. J. Natt, A. M. Witkowska, and E. Lingafelter, Acta Crystallogr. **22**, 775 (1967).
[68] J. Do, X. Wang, and A. J. Jacobson, J. Solid State Chem. **143**, 77 (1999).